Development of a real-time on-road emission (ROE v1.0) model for street-scale air quality modeling based on dynamic traffic big data

Luolin Wu[1], Ming Chang[2], Xuemei Wang[2], Jian Hang[1], Jinpu Zhang[3]

[1]School of Atmospheric Sciences, Sun Yat-sen University, Guangzhou 510275, P. R. China

5 [2]Institute for Environmental and Climate Research, Jinan University, Guangzhou 510632, P. R. China

[3]Guangzhou Environmental Monitoring Center, Guangzhou 510030, P. R. China

Correspondence to: Xuemei Wang (eciwxm@jnu.edu.cn)

Abstract. Rapid urbanization in China has led to heavy traffic flows in street networks within cities, especially in eastern China, the economically developed region. This has increased the risk of exposure to vehicle-related pollutants. To evaluate

10 the impact of vehicle emissions and provide an on-road emission inventory with higher spatial–temporal resolution for street-network air quality models, in this study, we developed the Real-time On-road Emission (ROE v1.0) model to calculate street-scale on-road hot emissions by using real-time big data for traffic provided by the Gaode map navigation application. This Python-based model obtains street-scale traffic data from the map application programming interface (API), which are open-access and updated every minute for each road segment. The results of application of the model to Guangzhou, one of the three

15 major cities in China, showed on-road vehicle emissions of carbon monoxide (CO), nitrogen oxide (NO_x), hydrocarbons (HC), PM_{10}, and $PM_{2.5}$ to be 35.22×10^4 Mg/a, 12.05×10^4 Mg/a, 4.10×10^4 Mg/a, 0.49×10^4 Mg/a, and 0.55×10^4 Mg/a, respectively. The spatial distribution reveals that the emission hotspots are located in some highway-intensive area and suburban town centers. Emission contributions show that the dominant contributors are light-duty vehicles (LDVs) and heavy-duty vehicles in urban areas and LDVs and heavy-duty trucks in suburban areas, indicating that the traffic control policies regarding duty

20 trucks in urban areas are effective. In this study, the Model of Urban Network of Intersecting Canyons and Highways (MUNICH) was applied to investigate the impact of traffic volume change on street-scale photochemistry in the urban area by using the on-road emission results from the ROE model. The modeling results indicate that the daytime NO_x concentrations on national holidays are 26.5% and 9.1% lower than those on normal weekdays and normal weekends, respectively. Conversely, the national holiday O_3 concentrations exceed normal weekday and normal weekend amounts by 13.9% and 10.6%,

25 respectively, owing to changes in the ratio of emission of VOCs and NO_x. Thus, not only the on-road emission, but other emissions should be controlled in order to improve the air quality in Guangzhou. More significantly, the newly developed ROE model may provide promising and effective methodologies for analyzing real-time street-level traffic emissions and high-resolution air quality assessment for more typical cities or urban districts.

1 Introduction

30 With rapid economic development and urbanization, the number of vehicles in use in China has grown in recent years (National Bureau of Statistics of China, 2017). As one of the three major city clusters, the Pearl River Delta (PRD) region, or its main city, Guangzhou, has seen significant increase in the number of vehicles, a phenomenon that has become the dominant contributor to carbon monoxide (CO), nitrogen oxide (NO_x), and hydrocarbon (HC) emissions (He et al., 2002; Zheng et al., 2009b), and have thus brought about more frequent and more severe public health problems in Chinese megacities (An et al.,

35 2013). Previous studies have shown that on-road vehicle emissions can contribute approximately 22–52% of the total CO, 37–47% of the NO_x, and 24–41% of the HC detected in cities (Zhang et al., 2009; Zheng et al., 2014, 2009a; Li et al., 2017).

Numerical air quality modeling can be considered an effective method to estimate on-road vehicle emissions and control their effect on the urban air quality (Wang and Xie, 2009; He et al., 2016). For this purpose, a realistic on-road vehicle emission

inventory should be developed as the pollutant source input data. The two main methodologies used in recent years to establish such an inventory are top-down and bottom-up techniques.

Top-down methods, such as that used in the MOBILE model offered by the US Environmental Protection Agency (EPA) or other similar macroscale models, require the vehicle population, vehicle kilometers travelled (VKT), and mean vehicle

5 speed of the entire city data to first calculate the total amount of vehicular emissions. Then, it allocates the emissions to each grid cell utilizing parameters such as the road density and road hierarchy (Saide et al., 2009; Jing et al., 2016; Liu et al., 2018). Many studies have adopted this method to develop city- or national-level vehicle emission inventories in China (Hao et al., 2000; Cai and Xie, 2007; Guo et al., 2007; Saide et al., 2009; Zheng et al., 2009b; Sun et al., 2016). However, the top-down inventories offer low-level spatial and temporal resolution because of the allocation method and input data. Generally, the

10 spatial allocation of the top-down inventories is based on the road network. The higher the road density and length are, the greater is the amount of emission in the same grid. This allocation method simplifies the road emissions by assuming that every road of a specific road type (e.g., highway, artery road, and local road) experiences the same traffic volume no matter where it is located. In addition, the emission factors used under the same traffic speed in the entire city also leads to inaccurate results for the inventory. Moreover, for some megacities (e.g., Guangzhou), there are traffic control policies in place in some

15 specific urban areas that imply emissions should be different in these areas. Besides, the VKT data are usually given on the scale of years, which limits the temporal resolution of the inventory. For numerical modeling, the accuracy of the emission inventory may have a great impact on the simulation result because of the heavy reliance of numerical models on the emission inventory (Jing et al., 2016). This scale of the emission inventory may not reflect the real emission conditions for the on-road vehicles within the city, which does not lead to effective evaluation of traffic-related impact on air pollution in a complex

20 situation such as street-level traffic flow (Huo et al., 2009).

Consequently, several studies have established higher-resolution inventories using the bottom-up approach. The main difference in this method is that bottom-up inventories are based on information from the road segment. Therefore, spatial distribution is directly obtained from the input data and there is no need for spatial and temporal allocation. Among the input data, the traffic data are crucial for establishing the inventories and determining their accuracy. Some previous studies have

25 used traffic simulation models to obtain the traffic speed or volume data within road networks (Pallavidino et al., 2014; Zhang et al., 2016; Chen et al., 2017; Ibarra-Espinosa et al., 2018). Based on the traffic model, the method could provide traffic data for each road from low-resolution average data. However, the results from such traffic models may not reflect the realistic situation quite well, which would reduce the accuracy of the inventories. Many other studies have used realistic traffic data, which are road-side or the on-board observation data obtained at certain road segments, to establish inventories and improve

30 their accuracy (Huo et al., 2009; Wang et al., 2008, 2010; Wang and Xie, 2009; Yao et al., 2013). Although the observed traffic data are helpful for inventory establishment, their limitation is obvious in that large-scale observation for a whole city requires extensive human and material resources, which are expensive and time consuming. Besides, such observation may not provide real-time traffic data, which reduces the temporal resolution for the inventories.

Nowadays, with the development of the image identification technology and other observation detectors, realistic traffic

35 data can be obtained easily from the road network. The extensive implementation of closed circuit televisions and other detection subsystems in the city helps in the application of the intelligent transport system (ITS) in China (Wu et al., 2009), making it possible to attain city-scale real-time traffic data. By using the ITS traffic data, many previous studies have successfully developed inventories for different areas in China (Jing et al., 2016; Liu et al., 2018; Zhang et al., 2018). Such studies provided us a new direction for the establishment of bottom-up inventories. The real-time traffic data from the road

40 network could be the most precise input data for on-road emission inventories and could significantly improve the spatial and temporal resolution of the inventories. However, there are still some difficulties in using the ITS data. In some cities, construction of the ITS is not complete yet or has not even been carried out. Moreover, the inconsistency of the data standards leads to an inefficient way of data utilization (Zhang, 2010). Furthermore, the low degree of the data sharing may be the biggest barrier to using traffic data obtained from the ITS (Huang et al., 2017).

45 With the help of a high-resolution emission inventory, numerical models can assess the impact of on-road vehicle emissions on the air quality (Huo et al., 2009). The flow and air quality modeling in cities are commonly categorized into four

groups by the length scales, i.e., street scale (~100 m), neighborhood scale (~1 km), city scale (~10 km), and regional scale (~100 km) (Britter and Hanna, 2003). As reviewed earlier (Zhang et al., 2012), regional-scale chemical transport models (CTMs) have been widely applied for investigating the chemistry and transport of air pollutants from their emission source. Many studies have successfully revealed that on-road vehicles are the main contributors of the air pollutants in the regional scale (~100 km) in urban areas using regional-scale CTMs (Che et al., 2011; Saikawa et al., 2011; He et al., 2016; Ke et al., 2017). In addition, some researchers have investigated street-scale and neighborhood-scale pollutant dispersion and urban air quality by adopting computational fluid dynamics (CFD) models (Fernando et al., 2010; Kim et al., 2012; Kwak et al., 2013; Kwak and Baik, 2014; Park et al., 2015; Zhong et al., 2016). City-scale (~10 km) CFD modeling, however, usually requires billions of grids because a city may include tens of thousands of buildings with a high-resolution complex street network (Di Sabatino et al., 2008; Ashie and Kono, 2011). Thus, as city-scale CFD simulations are very expensive and time consuming, they are currently rare. Recently, some models have been developed and applied to investigate street-level air quality at the city scale (Davies et al., 2007; Righi et al., 2009; Zhang et al., 2016; Kim et al., 2018) by balancing the requirements of high resolution and low computational costs.

In this direction, the first purpose of this study was to find a new, open-access source of real-time and high-quality traffic data that could be the input for developing an on-road emission inventory with high spatial and temporal resolution for cities or urban districts. For initial application of this method, Guangzhou was selected as the target city for the work not only because of the large number of vehicles in use there, but also because of its well-developed ITS, owing to the 2010 Asian Games (Xiong et al., 2010), which enables evaluation of this method. The Real-time On-road Emission (ROE v1.0) model, a Python-based on-road emission model, was developed in this study for utilizing these traffic data to establish the bottom-up on-road emission inventory. Finally, a street-level chemistry transport model was used to apply the emission results and study the impact of traffic volume variations on the air quality in the urban districts of Guangzhou.

2 Description of ROE model

2.1 Model structure

To calculate on-road vehicle emissions from real-time traffic data, the ROE model was developed: the model structure is shown in Figure 1. The model, which has been implemented in Python 3, can be divided into four parts: crawler, preprocessing, emission calculation, and output modules. (1) The crawler module crawls real-time traffic data from the ITS, Internet, or any other data source only if the user updates the code to fit the format of the data source. Before running the module, the area of study should be set in the module and the coordinate transformation script should be activated in case the coordinates are different. (2) The preprocessing module is used for fitting the time frequency between the data source and the air quality modeling system. Subsequently, the traffic volume data are also calculated from the traffic speed data in this module. (3) The emission calculation module uses traffic information from the preprocessing module and information about vehicle fleets to calculate emissions for each street segment using the following equation:

$$E_{s,t} = \sum EF_{s,v} \times V_{v,t} \times L, \tag{1}$$

where $E_{s,t}$ is the emission of pollutant s at time t (g/h); $EF_{s,v}$ is the emission factor of pollutant s for vehicle category v (g/km); $V_{v,t}$ is the traffic volume of the vehicle (i.e., the number of vehicles, veh) category v at time t (veh/h); and L is the length of the street segment (km). The total emission in one specific area is given by the sum of emissions in every street segment within the area. (4) The output module sums up all the information given by the emission calculation module and can be modified to provide all the results produced during the emissions calculation. In addition, there is a tool that can modify the format of emissions in the ROE model, making it possible to provide the on-road emissions to other air quality models.

Geoscientific
Model Development
Discussions

2.2 Emission factors

In this study, vehicle emission factors offered by the Ministry of Ecology and Environment of the People's Republic of China (MEP) were adopted to calculate the emission from vehicles on road (MEP, 2014). Besides, the emission factors of liquefied petroleum gas (LPG) vehicles were taken from a previous study completed in Guangzhou (Zhang et al., 2013). According to the MEP guide, vehicles are classified as one of the following: a light-duty vehicle (LDV), a middle-duty vehicle (MDV), a heavy-duty vehicle (HDV), a light-duty truck (LDT), a middle-duty truck (MDT), a heavy-duty truck (HDT), a motorcycle (MC), a taxi, or a bus. The fuel type is classified as petrol, diesel, or other (such as liquefied petrol gas or natural gas). The emission standard is classified as Pre-China I, China I, China II, China III, China IV, or China V. In addition, the correction factors involving environmental conditions (e.g., temperature, relative humidity, and altitude) and traffic conditions obtained from the technical guide were also considered in the study. For the HC, moreover, the evaporation of petrol was also considered during the emission calculation. The factor of the evaporation was also taken from the MEP guidebook.

2.3 Traffic data from floating car

In this study, the traffic speed data of each street segment were obtained from *amap.com* (also called Gaode map), a widely adopted map application in China (Figure 2). Based on the GPS and mobile network information, the vehicle speed and location information were collected from the map user's devices while using the map navigation on the road. These data are updated in real time and can be used through the application programming interface (API). Because of the data being updated in real time, the emission data can be also renewed in real time.

However, the map application could not provide the traffic volume data directly. Many studies have shown that the traffic volume can be estimated by the average traffic speed based on the relationship between the speed and the volume of traffic (Wang, 2003; Kuo and Tang, 2011; Xu et al., 2013; Yao et al., 2013; Hooper et al., 2014; Jing et al., 2016). There are many speed–flow models and each of them has certain advantages and disadvantages. In this study, the Underwood volume calculation model (Underwood, 1961) was selected to retrieve the volume information because of its successful application in China (Jing et al., 2016). The model is described by Eq. (2):

$$V = k_m u \ln \frac{u_f}{u}, \tag{2}$$

where V is the traffic volume at speed u (veh/h); k_m is the traffic density (veh/km); u is the traffic speed (km/h); and u_f is the free speed (km/h). In the Underwood model, k_m and u_f are given by fitting the model based on observation data obtained at the roadside and video identification data gained from different road types (Zheng et al., 2009b; Jing et al., 2016; Liu et al., 2018).

To calculation the traffic volume of national highways, another speed–flow model was used based on an observation-based study undertaken in China (Wang, 2003). This model is described as follows:

When the speed limit is 120 km/h,

$$V = -0.611u^2 + 73.320u; \tag{3}$$

when the speed limit is 100 km/h,

$$V = -0.880u^2 + 88.000u; \tag{4}$$

when the speed limit is 80 km/h,

$$V = -1.250u^2 + 100.000u; \tag{5}$$

when the speed limit is 60 km/h,

$$V = -2.000u^2 + 120.000u; \tag{6}$$

where V is the traffic volume at speed u (veh/h) and u is the traffic speed (km/h).

Because of the traffic control policy in Guangzhou, the whole city is divided into two areas: the urban area and the suburban area (Figure 3). Therefore, the traffic volume is also calculated accordingly (Figure 4). The traffic control policies in urban areas mainly includes the following points: (1) No truck is allowed to enter the urban area in the morning (7:00–9:00) and evening (18:00–20:00) rush hours; (2) No middle- and heavy-duty truck is permitted to enter the urban area during the

daytime (7:00–22:00); (3) No non-local truck can enter the urban area during the daytime (7:00–22:00); (4) No motorcycle can enter the urban area, either.

2.4 Vehicle fleet information

The figures for each vehicle classification was taken from the Statistical Yearbook of Guangzhou (Figure 5(a)) (Guangzhou

5   Bureau of Statistics, 2017). As for the emission standard (Figure 5(b)) and fuel type data (Figure 6) of the vehicle, they were given by a previous study undertaken in Guangzhou (Zhang et al., 2013, 2015).

3 The description of street-level air quality model

For evaluating the impact of on-road emissions on air quality at the street level in Guangzhou, an air quality model called the Model of Urban Network of Intersecting Canyons and Highways (MUNICH) was employed in this study with the on-road

10   emission results from the ROE model. MUNICH is a street-network CTM that includes street-canyon and street-intersection components in the model (Kim et al., 2018).

In this study, the Weather Research and Forecasting (WRF) model (Skamarock et al., 2008) was used to provide the meteorological data (including the wind profile, boundary layer height, and friction velocity) for the modeling. The WRF simulation was conducted with four nested domains at resolutions of 27 km, 9 km, 3 km, and 1 km (Figure 7a). The physical

15   scheme is listed in Table 1.

In the MUNICH, the CB05 chemical kinetic mechanism (Yarwood et al., 2005) is used to simulate the photochemical reaction at street-level for an urban street network. For the MUNICH run, the model was applied to simulate pollutants dispersion in the Tianhe District, the urban downtown of Guangzhou. As the simulation area, 31 main street segments were selected for simulating the variation in the concentrations of pollutants.

20   The urban morphology data for the building height were obtained from the WUDAPT dataset (Ching et al., 2018) and the street data were given by the OpenStreetMap dataset (https://www.openstreetmap.org/). The street length data were calculated directly from the location of the start and end intersections of each street segment. For the street width, the data were retrieved from the feature class of the road and the width of each lane was assumed to be 3.5 m.

The simulation period in the study was from the 28th April 2018 to the 2nd May 2018, with another 3-day spin-up time

25   before this period.

The observed concentration data for NO_2 and O_3 for the boundary conditions and modeling evaluation during the simulation period were obtained from the Guangzhou Environmental Monitoring sites near (YangJi site, YJ) and inside (Tiyuxi site, TYX) the simulation area (Figure 7c).

4 Application of ROE model to Guangzhou

30   **4.1 On-road emission inventory from ROE model**

4.1.1 Overview of the emission inventory

Using the high-resolution spatial and temporal traffic data from the map application, the emission inventory of on-road vehicles from the ROE model was established for this study. Table 2 shows the annual emissions from vehicles within the Guangzhou city compared with two other gridded emission inventories in China: the MEIC model (http://meicmodel.org/) and a PRD

35   region local emission inventory (Zheng et al., 2009a). The annual total on-road emissions in this study were 35.22×10^4 Mg/a of CO, 12.05×10^4 Mg/a of NO_x, 4.10×10^4 Mg/a of HC, 0.49×10^4 Mg/a of $PM_{2.5}$, and 0.55×10^4 Mg/a of PM_{10}. Because of the shorter total road length and traffic control policies in urban areas (Figure 3), the urban on-road emissions of CO, NO_x,

HC, $PM_{2.5}$, and PM_{10} were only 13.1%, 8.8%, 12.7%, 8.2%, and 9.1% of the total on-road emissions, respectively, suggesting that the suburban area is the dominant area for on-road emissions in Guangzhou.

As shown in Table 3, the emission contribution of local roads in urban areas is the most important component because of the length of local road, which is 5.4 times and 4.8 times of that of highways and artery roads in urban areas, respectively. Although the length of the highway is shorter, the traffic volume on the highway is much more than that on the local road (Figure 4), which leads to the highest contribution of emissions arising from the suburban area. Besides, the emission contributions from urban and suburban areas are different on weekdays and weekends. In urban areas, the daily total emissions are 129.94 Mg/d and 118.29 Mg/d of CO, 30.15 Mg/d and 27.71 Mg/d of NO_x, 14.74 Mg/d and 13.40 Mg/d of HC, 1.27 Mg/d and 1.16 Mg/d of $PM_{2.5}$, and 1.41 Mg/d and 1.29 Mg/d of PM_{10} on the weekday and weekend, respectively. In suburban areas, the total emissions on the weekday and weekend are 873.97 Mg/d and 758.41 Mg/d of CO, 315.10 Mg/d and 267.91 Mg/d of NO_x, 102.46 Mg/d and 88.22 Mg/d of HC, 13.01 Mg/d and 10.98 Mg/d of $PM_{2.5}$, and 14.45 Mg/d and 12.19 Mg/d of PM_{10}, respectively. The total respective emissions of CO, NO_x, HC, $PM_{2.5}$, and PM_{10} on a weekday are 114.5%, 116.8%, 115.3%, 117.6%, and 117.7% of the values on a weekend, respectively.

4.1.2 Spatial distribution of emissions

Due to the vehicle activities, the spatial distribution of on-road emissions was consistent with the structure of the street network. For a better description of this spatial distribution, the emissions were mapped into a 1-km-resolution fishnet and the total emission was the sum of the on-road emissions from all the grid cells. The distribution of each pollutant is shown in Figure 8. Overall, the high-value grid cells were generally along the highway. In suburban areas, high-value areas away from the highway and artery road normally denoted suburban town centers that had more local roads. In urban areas, the high-value areas were more closely related to the density of the urban local road. The emission hotspots were less prominent in urban areas than those in suburban areas due to the strict traffic control policies. The spatial distribution indicated that the next effective control policy of on-road emissions should pay more attention to the control of vehicles in suburban areas.

4.1.3 Emission contributions of vehicles by their classification

The different emission contributions of different vehicle classifications in urban and suburban areas are shown in Figure 9. Because LDVs accounted for the largest number, their emission contribution was the dominant proportion of total emissions in urban areas for each pollutant. The contribution percentages of CO, HC, NO_x, $PM_{2.5}$, and PM_{10} were 80.9%, 84.1%, 26.4%, 38.3%, and 38.2%, respectively. The second largest contributor to the on-road emissions was HDVs, at percentages of 5.8%, 2.9%, 30.3%, 35.2%, and 35.2% for CO, HC, NO_x, $PM_{2.5}$, and PM_{10}, respectively. As for the buses, except for the contribution of NO_x, which accounted for 20.3% of the emissions, the proportion of other pollutants was less than 2% because of the use of LPG. In the case of trucks, the total contribution of LDTs, MDTs, and HDTs were 10.3%, 9.3%, 21.2%, 23.3%, and 23.3% for CO, HC, NO_x, $PM_{2.5}$, and PM_{10}, respectively, with the traffic control policies in place in the urban area. The taxi contribution was less than 1% because of the small number of taxis and their use of LPG. In suburban areas, the dominant contributor of CO and HC emissions was the LDV because of its abundance. For the NO_x, $PM_{2.5}$, and PM_{10}, however, the HDT provided the largest contribution at 36.5%, 43.2%, and 43.3%, respectively. Besides, LDVs, HDVs, and buses were also important contributors of NO_x, at 19.4%, 17.4%, and 10.7%, respectively. As for particulate matter, the respective percentage of emissions (for both PM_{10} and $PM_{2.5}$) owing to LDVs, HDVs, and LDTs were 19.7%, 20.5%, and 9.0%, suggesting these vehicles were also important sources of both $PM_{2.5}$ and PM_{10}.

4.2 Application of ROE model results in street-level air quality model

4.2.1 Modeling evaluation in urban area of Guangzhou

During the simulation period, the model results were evaluated for the TYX observation site inside the street network. The on-road emissions were provided by the ROE model discussed previously. Street segments providing high NO_x emission

5   values also provided high HC emissions because of the positive relationship between traffic volume and on-road emissions as shown in Figure 10.

    The time series for simulated NO_2 and O_3 within the street network were compared with observed concentrations (Figure 11). The performance statistics for NO_2 and O_3 are shown in Table 4. Here, the statistical measures such as observation (OBS) mean, simulation (SIM) mean, the mean bias (MB), the normalized mean bias (NMB), the normalized

10   mean error (NME), the mean relative bias (MRB), the mean relative error (MRE), the root mean squared error (RMSE), and the correlation coefficient (CORR) were used for modeling validation. For NO_2, the model overestimated values, with a MB value of 4.7 $\mu g/m^3$. The respective values of NMB, NME, MRB, MRE, RMSE, and CORR were 15.2, 68.8, 3.0, 3.2, 25.7, and 0.90. However, the model underestimated O_3 values, with a MB value of –1.6 $\mu g/m^3$. The values of NMB, NME, MRB, MRE, RMSE, and CORR were –2.7, 24.3, <0.1, 0.3, 18.7, and 0.80, respectively. Overall, since only on-road emissions are

15   considered in the modeling domain, the model gives good performance for the simulation and can be applied in the further study of the impact of on-road vehicles on the air quality.

4.2.2 Impact of traffic volume variations on air quality

To investigate how traffic volume change affects the air quality at the street level, a Chinese national holiday was chosen as

20   the target simulation period for the modeling. Figure 12 shows the diurnal variation of the traffic volume during the national holiday, normal weekday, and normal weekend before and after the holiday in the simulation street network. On the normal weekday, two typical rush hour trends appeared during the 8:00–10:00 and 17:00–19:00 periods (although 28th April was a Saturday, it was still a normal workday to compensate for the holiday). For the normal weekend and the national holiday, the peak of the traffic volume was noted between 14:00 and 16:00 and there was no rush hour peak on these days. At nighttime,

25   not much difference was noted for the traffic volumes on the normal weekday, the normal weekend, and the national holiday, especially after midnight. However, the higher traffic volume between 21:00 and 23:00 on the 28th April at night may have been caused by people traveling out before the national holiday (e.g., going back home across the city or traveling to other places).

    To study how the traffic volume change affects the air quality in urban areas, three sensitivity cases were used as follows:

30   (1) in the national holiday case, the on-road emissions between 29th April and 1st May were used as the original emissions during the simulation period, which represents the base case; (2) in the normal weekday case, diurnal on-road emissions for three national holiday days were replaced by emissions of 28th April, (3) in the normal weekend case, the national holiday period emissions were replaced by the diurnal on-road emissions of 5th May. The diurnal variations of NO_x and O_3 in three cases are shown in Figure 13. During 0:00–5:00, because of similar traffic volume, there were no large differences in the NO_x

35   and the O_3 concentrations during this time. Because of the morning rush hour, the NO_x concentrations in the normal weekday case were much higher than those in the national holiday case in the morning. As Table 5 shows, the NO_x concentrations were 12.0–26.5% higher on the normal weekday case during this time. Even in the normal weekend case, simultaneously, the NO_x concentrations also went up by 9.1% higher than that on the national holiday in the morning, caused by people traveling for normal weekend engagements. In the afternoon, however, the difference between NO_x concentrations was less than 10% due

40   to the rising traffic volume on the national holiday. During the evening rush hour, although the traffic volume on the normal weekday was 1.3 times that of the national holiday, the maximum difference between NO_x concentrations was only 7.3%. This shows that the NO_x concentration variations are more affected by the boundary conditions (i.e., background concentration) in the evening.

Compared with the national holiday case, the O_3 concentrations were much lower in the normal weekday case. In the afternoon, when photochemical reactions are more prevalent, the national holiday O_3 concentrations exceed those on normal weekdays and weekends by 13.9% and 10.6%, respectively. This occurs because the simulation street network in the urban area is in the VOC-sensitive regime (Ye et al., 2016). The O_3 concentrations are positively correlated with the VOC emissions.
5   Because the NO_x emission amount was greater than the VOC emission amount, the reduction in NO_x, however, was also much higher than that of VOCs when the number of vehicles decreased on the national holiday. The larger NO_x emission reduction with lower VOC emission decrease led to a higher VOCs-to-NO_x emission ratio, which resulted in a higher O_3 concentration during the national holiday (Sanford and He, 2002).

5 Discussion and conclusions

10   The Real-time On-road Emission (ROE v1.0) model can provide the real-time and high-resolution emission inventories for the regional or street-level air quality model in China by using the real-world traffic information. The ROE model could provide the emission of CO, NO_x, HC, $PM_{2.5}$, PM_{10} or any other pollutants if these emission factors are included in the model. (This could be updated in subsequent releases.) As a result of utilization of the bottom-up method, the ROE model makes it possible to calculate the emissions in each street segment.
15   In this study, the traffic information of Guangzhou was obtained from the Gaode map, collected from map users while they are driving on the road. The geographic and speed information were taken from the map users' GPS devices and can be used through the map API. Using the ROE model and fully considering the traffic control policies in place in Guangzhou city, the annual total on-road emissions of CO, NO_x, HC, $PM_{2.5}$, and PM_{10} were modeled to be 35.22×10^4 Mg/a, 12.05×10^4 Mg/a, 4.10×10^4 Mg/a, 0.49×10^4 Mg/a, and 0.55×10^4 Mg/a, respectively. Spatial distribution shows that high-value hotspots of on-
20   road emissions are along the highway and suburban town center. Owing to the vehicle number and their distribution, LDVs constitute the dominant source of on-road emissions in Guangzhou. In suburban areas, however, the HDT is the most important contributor of NO_x, $PM_{2.5}$, and PM_{10}. Daily emissions of CO, NO_x, HC, $PM_{2.5}$, and PM_{10} on a weekday were found to be 14.5%, 16.8%, 15.3%, 17.6, and 17.7% more than the daily emissions on a weekend, respectively.
      Because of the high spatial and temporal resolution of the emission inventory from the ROE model, three sensitivity cases
25   were utilized to study the effect of vehicular on-road emissions on urban street-level air quality. On a national holiday, NO_x concentrations are 12.0–26.5% less than those on a normal weekday, since there is no morning rush hour on a holiday. Meanwhile, compared with the normal weekend, the NO_x concentrations on a national holiday also show a decrease of 9.1% in the peak value in the morning. However, reduction in the afternoon NO_x concentrations was smaller than that in the morning, suggesting that NO_x transportation from the surrounding boundaries is the main reason for the variation in the afternoon NO_x.
30   In addition, since the simulation street network is in the VOC-sensitivity regime, with the lower traffic on a national holiday and a normal weekend, the NO_x and VOC emissions are less than those on a normal weekday. However, the reductions in NO_x are higher than the decrease in VOC emissions, which leads to a higher VOCs-to-NO_x emission ratio and O_3 concentrations on a holiday and a normal weekend.
      Finally, the newly developed ROE model was confirmed to be effective for analyzing real-time city-scale traffic emissions
35   and perform high-resolution air quality assessment in street networks of Guangzhou city. The methodologies can be further extended to more typical cities or urban districts in China or other countries if the traffic information and emission factors are available for the model.

40   *Author contribution.* Luolin Wu and Xuemei Wang designed the experiments. Luolin Wu developed the model code and performed the simulations. Ming Chang organized and visualized the data. Jinpu Zhang collected and organized the observation data. Luolin Wu and Jian Hang prepared the manuscript with contributions from all co-authors.

Code availability. The python source code of the ROE v1.0 model and examples are available on Github (https://github.com/vnuni23/ROE, last access: 14 March 2019). More information and help are also available by contacting the authors.

5   *Competing interests.* The authors declare that they have no conflict of interest.

Reference

An, X., Hou, Q., Li, N. and Zhai, S.: Assessment of human exposure level to PM10 in China, Atmos. Environ., 70, 376–386,
15   doi:10.1016/j.atmosenv.2013.01.017, 2013.

Ashie, Y. and Kono, T.: Urban-scale CFD analysis in support of a climate-sensitive design for the Tokyo Bay area, Int. J. Climatol., 31(2), 174–188, doi:10.1002/joc.2226, 2011.

Britter, R. E. and Hanna, S. R.: Flow and dispersion in urban areas, Annu. Rev. Fluid Mech., 35(1), 469–496, doi:10.1146/annurev.fluid.35.101101.161147, 2003.

20   Cai, H. and Xie, S. D.: Estimation of vehicular emission inventories in China from 1980 to 2005, Atmos. Environ., 41(39), 8963–8979, doi:10.1016/j.atmosenv.2007.08.019, 2007.

Che, W., Zheng, J., Wang, S., Zhong, L. and Lau, A.: Assessment of motor vehicle emission control policies using Model-3/CMAQ model for the Pearl River Delta region, China, Atmos. Environ., 45(9), 1740–1751, doi:10.1016/j.atmosenv.2010.12.050, 2011.

25   Chen, R., Paristech, P. and Aguil, V.: A sensitivity study of road transportation emissions at metropolitan scale, J. Earth Sci. Geotech. Eng., 7(1), 151–173, 2017.

Ching, J., Mills, G., Bechtel, B., See, L., Feddema, J., Wang, X., Ren, C., Brorousse, O., Martilli, A., Neophytou, M., Mouzourides, P., Stewart, I., Hanna, A., Ng, E., Foley, M., Alexander, P., Aliaga, D., Niyogi, D., Shreevastava, A., Bhalachandran, P., Masson, V., Hidalgo, J., Fung, J., Andrade, M., Baklanov, A., Dai, W., Milcinski, G., Demuzere,
30   M., Brunsell, N., Pesaresi, M., Miao, S., Mu, Q., Chen, F. and Theeuwesits, N.: WUDAPT: An urban weather, climate, and environmental modeling infrastructure for the anthropocene, Bull. Am. Meteorol. Soc., 99(9), 1907–1924, doi:10.1175/BAMS-D-16-0236.1, 2018.

Davies, L., Bates, J. W., Bell, J. N. B., James, P. W. and Purvis, O. W.: Diversity and sensitivity of epiphytes to oxides of nitrogen in London, Environ. Pollut., 146(2), 299–310, doi:10.1016/j.envpol.2006.03.023, 2007.

35   Di Sabatino, S., Buccolieri, R., Pulvirenti, B. and Britter, R. E.: Flow and pollutant dispersion in street canyons using FLUENT and ADMS-Urban, Environ. Model. Assess., 13(3), 369–381, doi:10.1007/s10666-007-9106-6, 2008.

Fernando, H. J. S., Zajic, D., Di Sabatino, S., Dimitrova, R., Hedquist, B. and Dallman, A.: Flow, turbulence, and pollutant dispersion in urban atmospheres, Phys. Fluids, 22(5), 1–20, doi:10.1063/1.3407662, 2010.

Guangzhou Bureau of Statistics: Guangzhou Statistical Yearbook 2017, Guangzhou, People's Republic of China., 2017.

40   Guo, H., Zhang, Q., Shi, Y. and Wang, D.: On-road remote sensing measurements and fuel-based motor vehicle emission inventory in Hangzhou, China, Atmos. Environ., 41(14), 3095–3107, doi:10.1016/j.atmosenv.2006.11.045, 2007.

Hao, J., He, D., Wu, Y., Fu, L. and He, K.: A study of the emission and concentration distribution of vehicular pollutants in the urban area of Beijing, Atmos. Environ., 34(3), 453–465, doi:10.1016/S1352-2310(99)00324-6, 2000.

Geoscientific
Model Development
Discussions

He, J., Wu, L., Mao, H., Liu, H., Jing, B., Yu, Y., Ren, P., Feng, C. and Liu, X.: Development of a vehicle emission
inventory with high temporal-spatial resolution based on NRT traffic data and its impact on air pollution in Beijing -
Part 2: Impact of vehicle emission on urban air quality, Atmos. Chem. Phys., 16(5), 3171–3184, doi:10.5194/acp-16-
3171-2016, 2016.

5   He, K., Huo, H. and Zhang, Q.: Urban Air Pollution in China: Current Status, Characteristics, and Progress, J. Allergy Clin.
Immunol., 27, 397–431, doi:10.1146/annurev.energy.27.122001.083421, 2002.

Hooper, E., Chapman, L. and Quinn, A.: The impact of precipitation on speed–flow relationships along a UK motorway
corridor, Theor. Appl. Climatol., 117(1), 303–316, doi:10.1007/s00704-013-0999-5, 2014.

Huang, W., Wei, Y., Guo, J. and Cao, J.: Next-generation innovation and development of intelligent transportation system in
10   China, Sci. China Inf. Sci., 60(11), 1–11, doi:10.1007/s11432-017-9182-x, 2017.

Huo, H., Zhang, Q., He, K., Wang, Q., Yao, Z. and Streets, D. G.: High-Resolution Vehicular Emission Inventory Using a
Link-Based Method : A Case Study of Light-Duty Vehicles in Beijing, Environ. Sci. Technol., 43(7), 2394–2399, 2009.

Ibarra-Espinosa, S., Ynoue, R., O'sullivan, S., Pebesma, E., De Fátima Andrade, M. and Osses, M.: VEIN v0.2.2: an R
package for bottom-up vehicular emissions inventories, Geosci. Model Dev., 11(6), 2209–2229, doi:10.5194/gmd-11-
15   2209-2018, 2018.

Jing, B., Wu, L., Mao, H., Gong, S., He, J., Zou, C., Song, G., Li, X. and Wu, Z.: Development of a vehicle emission
inventory with high temporal-spatial resolution based on NRT traffic data and its impact on air pollution in Beijing -
Part 1: Development and evaluation of vehicle emission inventory, Atmos. Chem. Phys., 16(5), 3161–3170,
doi:10.5194/acp-16-3161-2016, 2016.

20   Ke, W., Zhang, S., Wu, Y., Zhao, B., Wang, S. and Hao, J.: Assessing the future vehicle fleet electrification: The impacts on
regional and Urban air quality, Environ. Sci. Technol., 51(2), 1007–1016, doi:10.1021/acs.est.6b04253, 2017.

Kim, M. J., Park, R. J. and Kim, J. J.: Urban air quality modeling with full O3-NOx-VOC chemistry: Implications for O3and
PM air quality in a street canyon, Atmos. Environ., 47(2), 330–340, doi:10.1016/j.atmosenv.2011.10.059, 2012.

Kim, Y., Wu, Y., Seigneur, C. and Roustan, Y.: Multi-scale modeling of urban air pollution: development and application of
25   a Street-in-Grid model (v1.0) by coupling MUNICH (v1.0) and Polair3D (v1.8.1), Geosci. Model Dev., 11(2), 611–629,
doi:10.5194/gmd-11-611-2018, 2018.

Kuo, C.-W. and Tang, M.-L.: Relationship among service quality, corporate image, customer satisfaction and behaviroal
intention for the elderly in high speed rail service, J. Adv. Transp., 47(June 2010), 512–525, doi:10.1002/atr, 2011.

Kwak, K. H. and Baik, J. J.: Diurnal variation of NOx and ozone exchange between a street canyon and the overlying air,
30   Atmos. Environ., 86(x), 120–128, doi:10.1016/j.atmosenv.2013.12.029, 2014.

Kwak, K. H., Baik, J. J. and Lee, K. Y.: Dispersion and photochemical evolution of reactive pollutants in street canyons,
Atmos. Environ., 70, 98–107, doi:10.1016/j.atmosenv.2013.01.010, 2013.

Li, M., Zhang, Q., Kurokawa, J. I., Woo, J. H., He, K., Lu, Z., Ohara, T., Song, Y., Streets, D. G., Carmichael, G. R., Cheng,
Y., Hong, C., Huo, H., Jiang, X., Kang, S., Liu, F., Su, H. and Zheng, B.: MIX: A mosaic Asian anthropogenic emission
35   inventory under the international collaboration framework of the MICS-Asia and HTAP, Atmos. Chem. Phys., 17(2),
935–963, doi:10.5194/acp-17-935-2017, 2017.

Liu, Y. H., Ma, J. L., Li, L., Lin, X. F., Xu, W. J. and Ding, H.: A high temporal-spatial vehicle emission inventory based on
detailed hourly traffic data in a medium-sized city of China, Environ. Pollut., 236, 324–333,
doi:10.1016/j.envpol.2018.01.068, 2018.

40   MEP: Technical Guide of Air Pollutant Emission Inventory for On Road Vehicles (Trial), Beijing, China., 2014.

National Bureau of Statistics of China: China Statistical Yearbook 2017, Beijing, People's Republic of China., 2017.

Pallavidino, L., Prandi, R., Bertello, A., Bracco, E. and Pavone, F.: Compilation of a road transport emission inventory for
the Province of Turin: Advantages and key factors of a bottom–up approach, Atmos. Pollut. Res., 5(4), 648–655,
doi:10.5094/APR.2014.074, 2014.

45   Park, S. J., Kim, J. J., Kim, M. J., Park, R. J. and Cheong, H. Bin: Characteristics of flow and reactive pollutant dispersion in
urban street canyons, Atmos. Environ., 108, 20–31, doi:10.1016/j.atmosenv.2015.02.065, 2015.

Righi, S., Lucialli, P. and Pollini, E.: Statistical and diagnostic evaluation of the ADMS-Urban model compared with an urban air quality monitoring network, Atmos. Environ., 43(25), 3850–3857, doi:10.1016/j.atmosenv.2009.05.016, 2009.

Saide, P., Zah, R., Osses, M. and Ossés de Eicker, M.: Spatial disaggregation of traffic emission inventories in large cities using simplified top-down methods, Atmos. Environ., 43(32), 4914–4923, doi:10.1016/j.atmosenv.2009.07.013, 2009.

5 Saikawa, E., Kurokawa, J., Takigawa, M., Borken-Kleefeld, J., Mauzerall, D. L., Horowitz, L. W. and Ohara, T.: The impact of China's vehicle emissions on regional air quality in 2000 and 2020: A scenario analysis, Atmos. Chem. Phys., 11(18), 9465–9484, doi:10.5194/acp-11-9465-2011, 2011.

Sanford, S. and He, D.: Some theoretical results concerning O3 -NOx -VOC chemistry and NOx -VOC indicators, J. Geophys. Res., 107(D22), 4659, doi:10.1029/2001JD001123, 2002.

10 Skamarock, W. C., Klemp, J. B., Dudhia, J., Gill, D. O., Barker, D. M., Duda, M. G., Huang, X.-Y., Wang, W. and Powers, J. G.: A description of the advanced research WRF version 3, NCAR Tech. Note NCAR/TN-475+ STR, 113 pp., 2008.

Sun, S., Jiang, W. and Gao, W.: Vehicle emission trends and spatial distribution in Shandong province, China, from 2000 to 2014, Atmos. Environ., 147(X), 190–199, doi:10.1016/j.atmosenv.2016.09.065, 2016.

Underwood, R. T.: Speed, volume, and density relationship: quality and theory of traffic flow, Yale Bur. Highw. Traffic,
15   141–188, 1961.

Wang, H., Chen, C., Huang, C. and Fu, L.: On-road vehicle emission inventory and its uncertainty analysis for Shanghai, China, Sci. Total Environ., 398(1–3), 60–67, doi:10.1016/j.scitotenv.2008.01.038, 2008.

Wang, H., Fu, L. and Chen, J.: Developing a high-resolution vehicular emission inventory by integrating an emission model and a traffic model: Part 2-a case study in beijing, J. Air Waste Manag. Assoc., 60(12), 1471–1475, doi:10.3155/1047-
20   3289.60.12.1471, 2010.

Wang, T. and Xie, S.: Assessment of traffic-related air pollution in the urban streets before and during the 2008 Beijing Olympic Games traffic control period, Atmos. Environ., 43(35), 5682–5690, doi:10.1016/j.atmosenv.2009.07.034, 2009.

Wang, W.: Practical speed-flow relationship model of highway traffic-flow (in chinese), J. SOUTHEAST Univ. Sci. Ed.,
25   33(4), 487–491, 2003.

Wu, J., Sui, Y. and Wang, T.: Intelligent transport systems in China, Proc. ICE - Munic. Eng., 162(1), 25–32, doi:10.1680/muen.2009.162.1.25, 2009.

Xiong, G., Wang, K., Zhu, F., Cheng, C., An, X. and Xie, Z.: Parallel traffic management for the 2010 Asian Games, IEEE Intell. Syst., 25(3), 81–85, doi:10.1109/MIS.2010.87, 2010.

30 Xu, F., He, Z., Sha, Z., Zhuang, L. and Sun, W.: Assessing the Impact of Rainfall on Traffic Operation of Urban Road Network, Procedia - Soc. Behav. Sci., 96, 82–89, doi:10.1016/j.sbspro.2013.08.012, 2013.

Yao, Z., Zhang, Y., Shen, X., Wang, X., Wu, Y. and He, K.: Impacts of temporary traffic control measures on vehicular emissions during the Asian Games in Guangzhou, China, J. Air Waste Manag. Assoc., 63(1), 11–19, doi:10.1080/10962247.2012.724041, 2013.

35 Yarwood, G., Rao, S., Yocke, M. and Whitten, G. Z.: Updates to the carbon bond chemical mechanism: CB05, Rep. RT-0400675, 246 pp.,. [online] Available from: http://www.camx.com/files/cb05_final_report_120805.aspx, 2005.

Ye, L., Wang, X., Fan, S., Chen, W., Chang, M., Zhou, S., Wu, Z. and Fan, Q.: Photochemical indicators of ozone sensitivity: application in the Pearl River Delta, China, Front. Environ. Sci. Eng., 10(6), 1–14, doi:10.1007/s11783-016-0887-1, 2016.

40 Zhang, F.: The current situation and development thinking of the intelligent transportation system in China, 2010 Int. Conf. Mech. Autom. Control Eng. MACE2010, 717, 2826–2829, doi:10.1109/MACE.2010.5536406, 2010.

Zhang, Q., Streets, D. G., Carmichael, G. R., He, K. B., Huo, H., Kannari, A., Klimont, Z., Park, I. S., Reddy, S., Fu, J. S., Chen, D., Duan, L., Lei, Y., Wang, L. T. and Yao, Z. L.: Asian emissions in 2006 for the NASA INTEX-B mission, Atmos. Chem. Phys., 9(14), 5131–5153, doi:10.5194/acp-9-5131-2009, 2009.

Zhang, S., Wu, Y., Liu, H., Wu, X., Zhou, Y., Yao, Z., Fu, L., He, K. and Hao, J.: Historical evaluation of vehicle emission control in Guangzhou based on a multi-year emission inventory, Atmos. Environ., 76, 32–42, doi:10.1016/j.atmosenv.2012.11.047, 2013.

5   Zhang, S., Wu, Y., Huang, R., Wang, J., Yan, H., Zheng, Y. and Hao, J.: High-resolution simulation of link-level vehicle emissions and concentrations for air pollutants in a traffic-populated eastern Asian city, Atmos. Chem. Phys., 16(15), 9965–9981, doi:10.5194/acp-16-9965-2016, 2016.

Zhang, S., Niu, T., Wu, Y., Zhang, K. M., Wallington, T. J., Xie, Q., Wu, X. and Xu, H.: Fine-grained vehicle emission management using intelligent transportation system data, Environ. Pollut., 241, 1027–1037, doi:10.1016/j.envpol.2018.06.016, 2018.

10   Zhang, Y., Bocquet, M., Mallet, V., Seigneur, C. and Baklanov, A.: Real-time air quality forecasting, part I: History, techniques, and current status, Atmos. Environ., 60, 632–655, doi:10.1016/j.atmosenv.2012.06.031, 2012.

Zhang, Y., Wang, X., Li, G., Yang, W., Huang, Z., Zhang, Z., Huang, X., Deng, W., Liu, T., Huang, Z. and Zhang, Z.: Emission factors of fine particles, carbonaceous aerosols and traces gases from road vehicles: Recent tests in an urban tunnel in the Pearl River Delta, China, Atmos. Environ., 122, 876–884, doi:10.1016/j.atmosenv.2015.08.024, 2015.

15   Zheng, B., Huo, H., Zhang, Q., Yao, Z. L., Wang, X. T., Yang, X. F., Liu, H. and He, K. B.: High-resolution mapping of vehicle emissions in China in 2008, Atmos. Chem. Phys., 14(18), 9787–9805, doi:10.5194/acp-14-9787-2014, 2014.

Zheng, J., Zhang, L., Che, W., Zheng, Z. and Yin, S.: A highly resolved temporal and spatial air pollutant emission inventory for the Pearl River Delta region , China and its uncertainty assessment, Atmos. Environ., 43(32), 5112–5122, doi:10.1016/j.atmosenv.2009.04.060, 2009a.

20   Zheng, J., Che, W., Wang, X., Louie, P. and Zhong, L.: Road-network-based spatial allocation of on-road mobile source emissions in the pearl river delta region, China, and comparisons with population-based approach, J. Air Waste Manag. Assoc., 59(12), 1405–1416, doi:10.3155/1047-3289.59.12.1405, 2009b.

Zhong, J., Cai, X. M. and Bloss, W. J.: Coupling dynamics and chemistry in the air pollution modelling of street canyons: A review, Environ. Pollut., 214, 690–704, doi:10.1016/j.envpol.2016.04.052, 2016.

25

Table 1. Physical parameterization configurations for WRF model

Physical parameterizations	
Microphysics Scheme	Morrison (2 moments)
Land-surface Scheme	Pleim-Xiu
Cumulus Scheme	Kain-Fristsch
Longwave Radiation Scheme	RRTM
Shortwave Radiation Scheme	Dudhia
Boundary-layer Scheme	ACM2
Urban Surface Scheme	UCM

30

Table 2. Annual on-road emissions in Guangzhou (unit: 10^4 Mg/year)

		CO	NO_x	HC	$PM_{2.5}$	PM_{10}
	Urban	4.61	1.07	0.52	0.04	0.05
This study	Suburban	30.61	10.98	3.58	0.45	0.50
	Total	35.22	12.05	4.10	0.49	0.55
MEIC-2016	(Gridded)	43.56	8.45	9.26	0.46	0.47

| PRD-2015 | (Gridded) | 28.89 | 6.99 | 4.65 | 0.52 | 0.52 |

Table 3. Daily emissions on different road type in urban and suburban area (unit: Mg/day)

		Road type	Length(km)	CO	NO_x	HC	$PM_{2.5}$	PM_{10}
weekday	urban	highway	301.87	9.71	3.15	1.02	0.11	0.12
		artery	337.19	17.24	4.95	1.88	0.19	0.21
		local	1629.92	102.99	22.05	11.84	0.97	1.08
	suburban	highway	2316.73	417.49	168.29	45.51	6.50	7.22
		artery	747.63	61.12	26.54	7.24	1.11	1.23
		local	8867.69	395.36	120.27	49.71	5.40	6.00
weekend	urban	highway	301.87	7.47	2.34	0.79	0.08	0.09
		artery	337.19	13.20	4.23	1.40	0.15	0.17
		local	1629.92	97.62	21.14	11.21	0.93	1.03
	suburban	highway	2316.73	428.30	156.78	47.14	6.07	6.74
		artery	747.63	59.20	26.56	6.99	1.10	1.22
		local	8867.69	270.91	84.57	34.09	3.81	4.23

5

Table 4 The performance statistics for NO₂ and O₃ in modeling (unit: μg/m³)

	Mean								
	OBS	SIM	MB	NMB	NME	MRB	MRE	RESE	CORR
NO_2	30.8	35.4	4.7	15.2	68.8	3.0	3.2	25.7	0.90
O_3	60.9	59.3	-1.6	-2.7	24.3	<0.1	0.3	18.7	0.80

Table 5. Daytime difference of NO_x compared to National holiday case

time	6:00	7:00	8:00	9:00	10:00	11:00	12:00	13:00	14:00	15:00	16:00	17:00	18:00	19:00	20:00
normal weekday	12.7%	21.7%	16.8%	26.5%	14.7%	12.0%	4.9%	0.6%	8.6%	2.2%	0.7%	0.2%	7.3%	5.9%	7.1%
normal weekend	-4.4%	0.1%	9.1%	6.7%	0.2%	7.0%	1.2%	2.6%	6.2%	0.8%	-0.6%	-0.9%	2.1%	-5.7%	4.9%

10   **Table 6. Daytime difference of O₃ compared to National holiday case**

| time	6:00	7:00	8:00	9:00	10:00	11:00	12:00	13:00	14:00	15:00	16:00	17:00	18:00	19:00	20:00
normal weekday	-4.5%	-15.7%	-52.8%	-48.9%	-37.5%	-25.9%	-15.6%	0.2%	-7.9%	-13.9%	-7.4%	-11.1%	-46.3%	-38.4%	-32.3%
normal weekend	2.9%	6.3%	-2.6%	-4.9%	-15.0%	0.5%	-4.0%	-1.6%	-5.7%	-10.6%	-0.4%	12.4%	-15.3%	-0.1%	3.7%
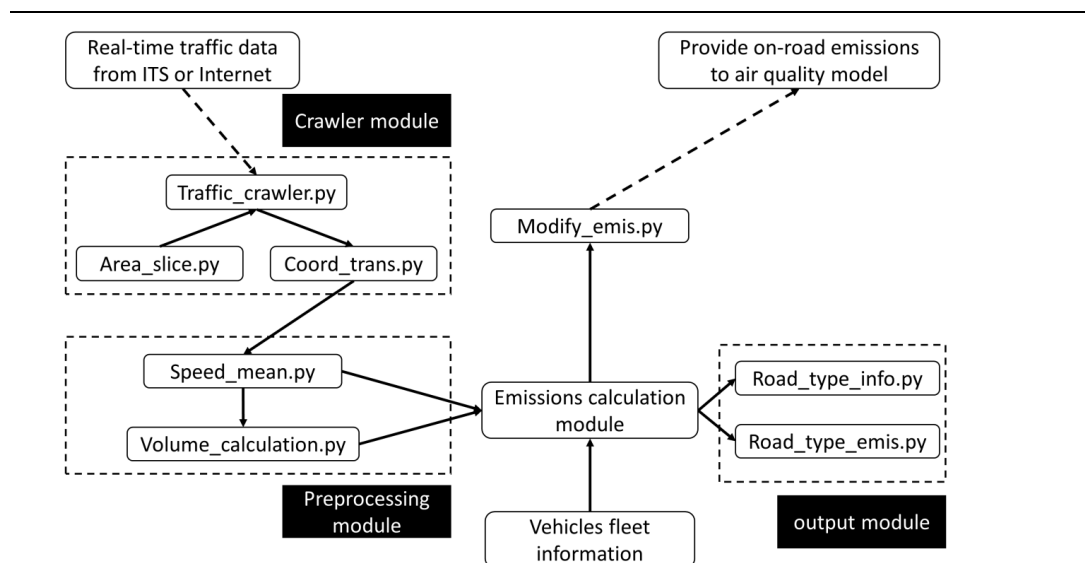
Figure 1. The structure of ROE model.
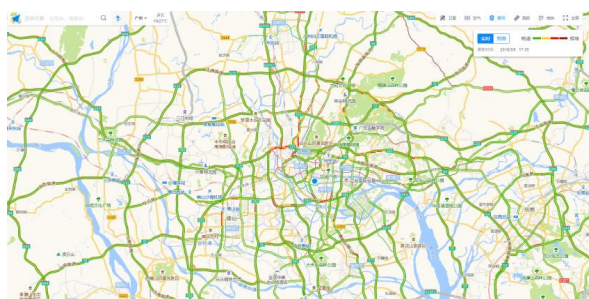
5   Figure 2. Traffic information from Gaode map.
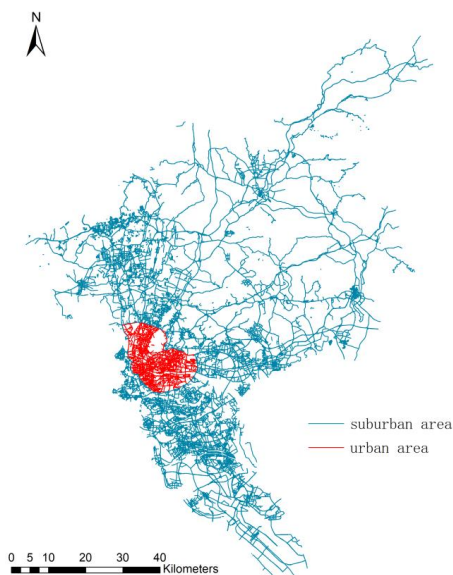
Figure 3. Traffic control area.
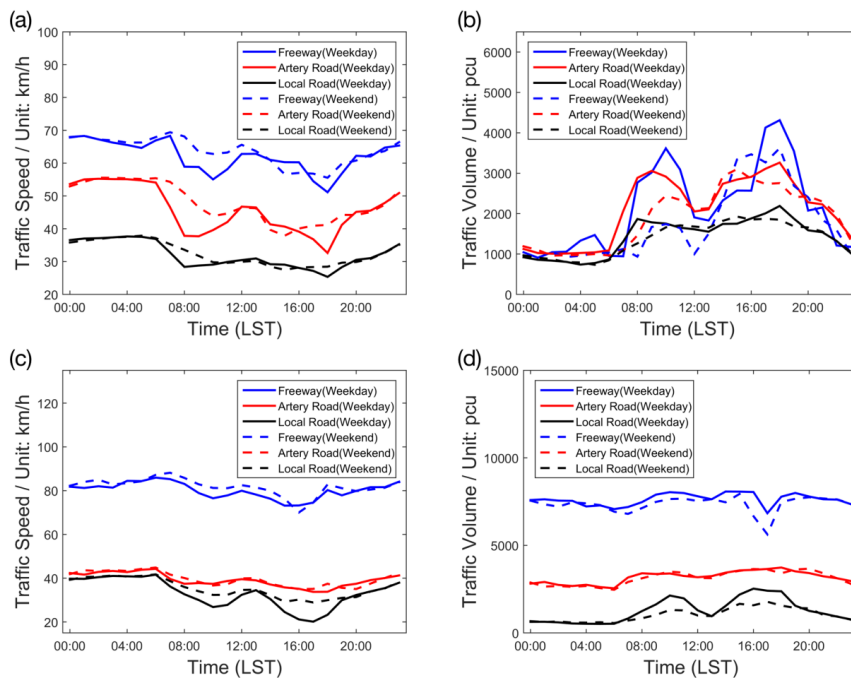
5   **Figure 4. Diurnal variation of average traffic speed and traffic volume in (a, b) urban area and (c, d) suburban area during
   weekday and weekend.**
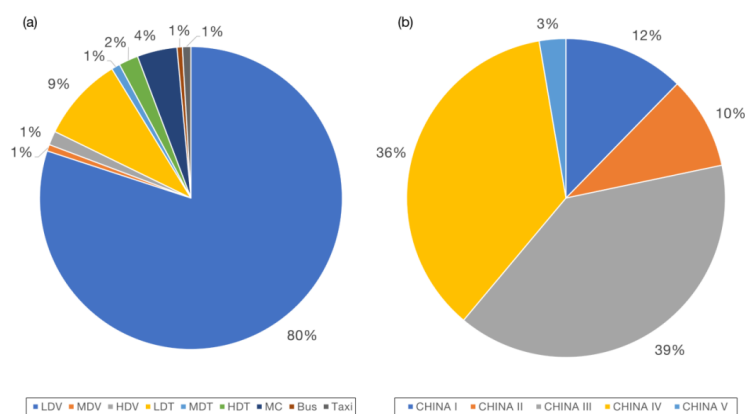
Figure 5. The percentage of (a) vehicle classification and (b) emission standard.
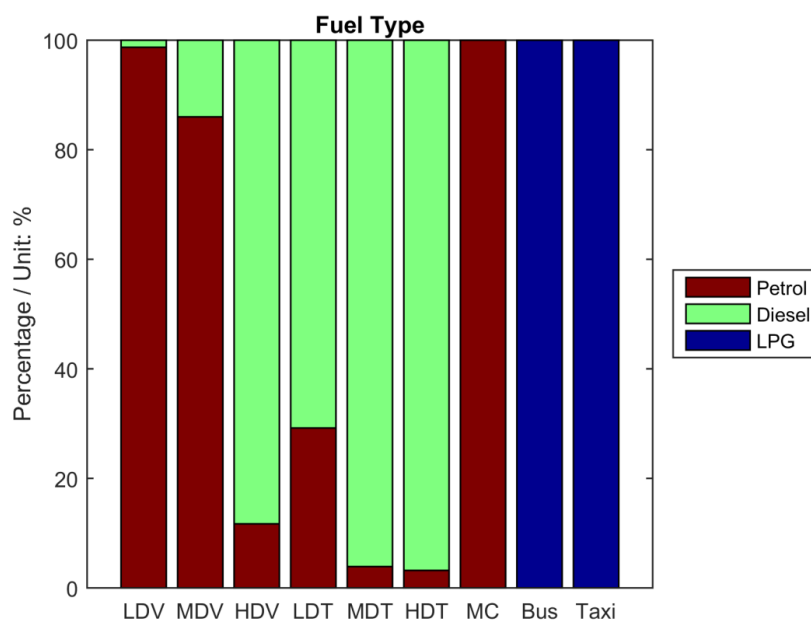
5   **Figure 6. Fuel type percentage of each vehicle classification.**

Geoscientific
Model Development
Discussions
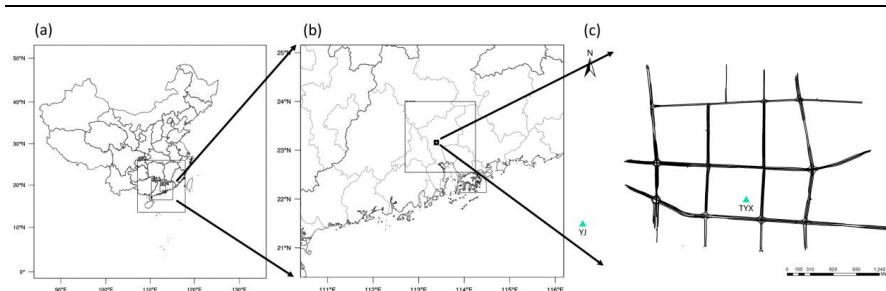
Figure 7. Simulation domain from regional scale to street-level scale: (a) four-nested simulation for WRF; (b) domains 3 and 4 covering the Pearl River Delta Region and Guangzhou city, the innermost box corresponds to the Tianhe District; (c) 31 street segments and two observation sites (triangle) within the MUNICH study domain.

5
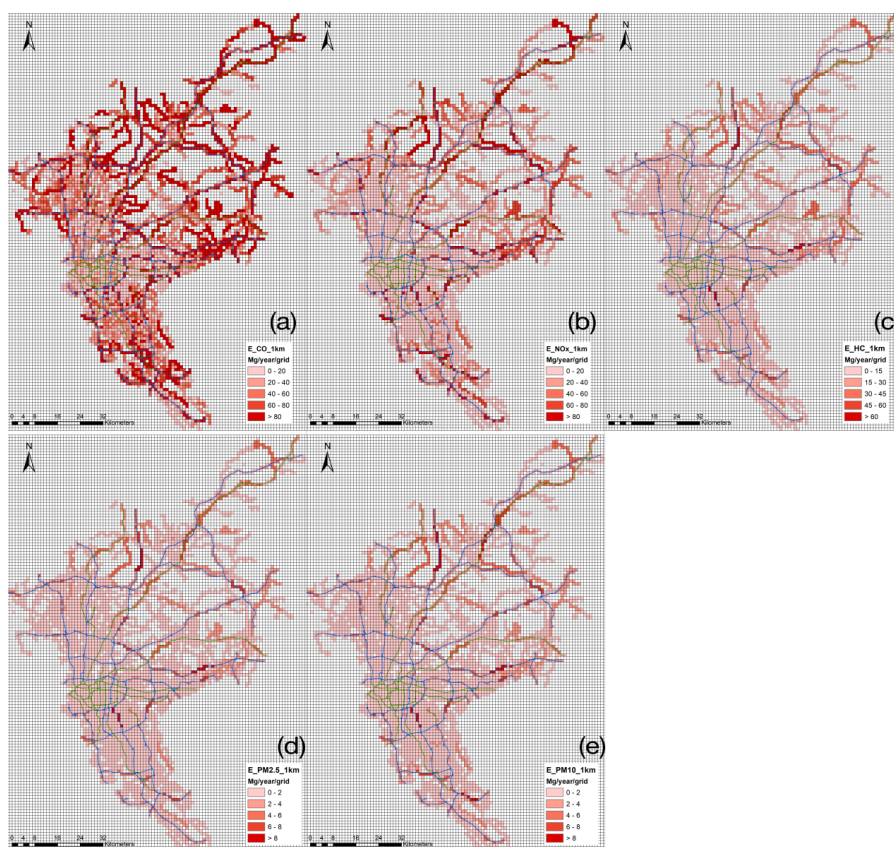
Figure 8. Spatial distribution of (a) CO, (b) NOₓ, (c) HC, (d) PM₂.₅, and (e) PM₁₀ from the on-road emissions in Guangzhou (blue lines: highways; green lines: arterial roads; local roads are not shown).
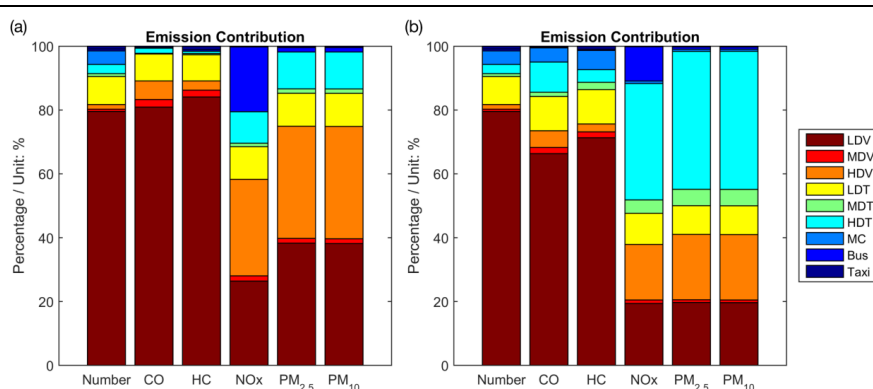
Figure 9. Emission contribution of each vehicle classification in (a) urban area and (b) suburban area.
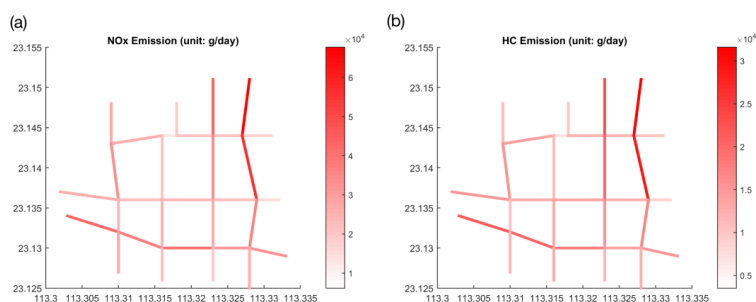
5   Figure 10. The spatial distribution of weekday (a) NOₓ and (b) HC emission in the simulated street network.
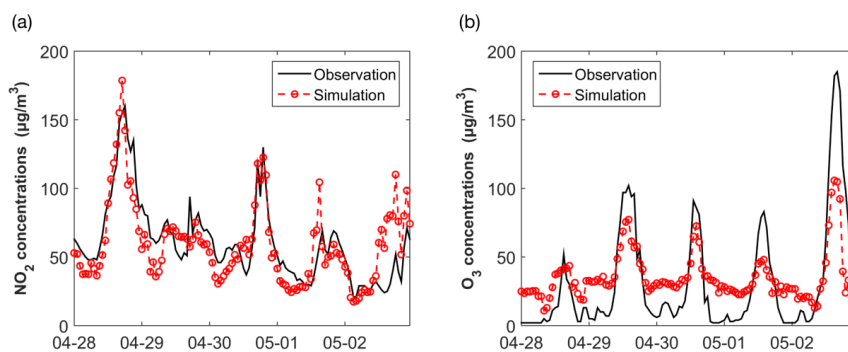
Figure 11. Time series of (a) NO₂ and (b) O₃ during the simulation period. (solid line: observation; dashed line: simulation).
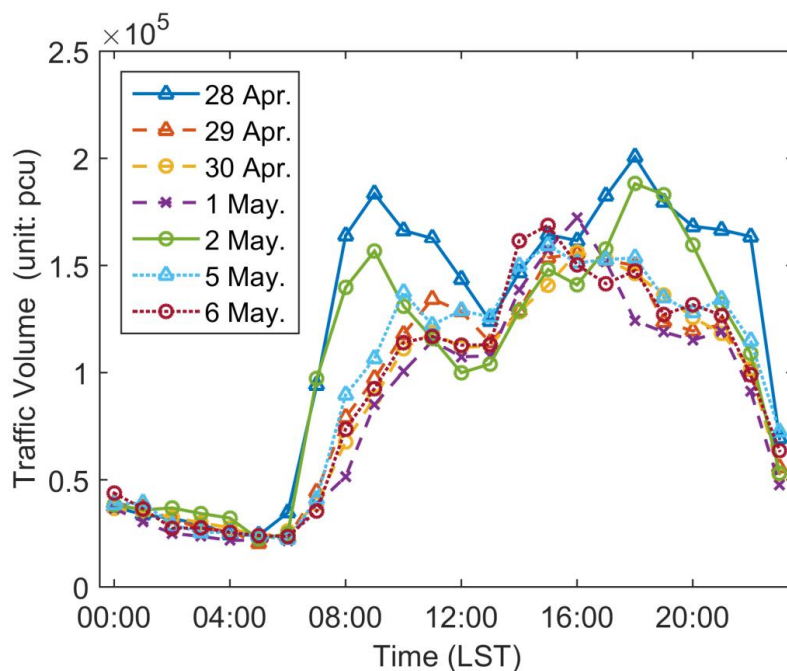
Figure 12. The diurnal variation of the total traffic volume in the simulation street network (solid line: normal weekday; dashed line: national holiday; dotted line: normal weekend).
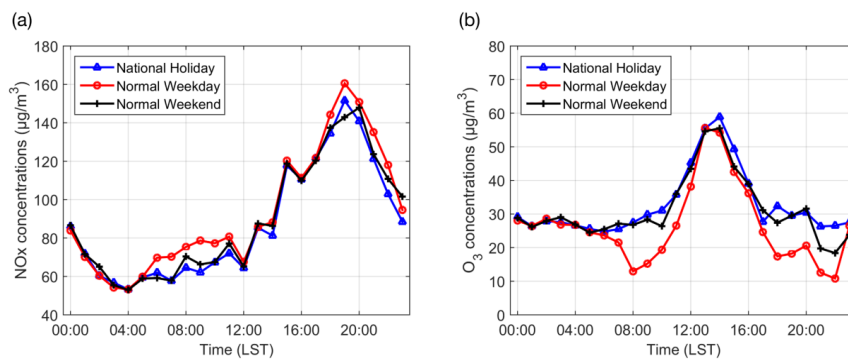
Figure 13. The (a) NOₓ and (b) O₃ diurnal variation of different sensitivity cases in the simulation street network

5